Composites Science and Technology 225 (2022) 109495

Contents lists available at ScienceDirect

Composites Science and Technology

journal homepage: www.elsevier.com/locate/compscitech

Innovative wicking and interfacial evaluation of carbon fiber (CF)/Epoxy composites by CF tow capillary glass tube method (TCGTM) with Tripe-CF fragmentation test

Jong-Hyun Kim [a,b], Dong-Jun Kwon [b], Lawrence K. DeVries [c], Joung-Man Park [a,b,c,*]

[a] Department of Materials Engineering and Convergence Technology, Gyeongsang National University, Jinju, 52828, Republic of Korea
[b] Research Institute for Green Energy Convergence Technology, Gyeongsang National University, Jinju, 52828, Republic of Korea
[c] Department of Mechanical Engineering, The University of Utah, Salt Lake City, UT, 84112, USA

ARTICLE INFO

Keywords:
CF tow Capillary glass tube method (TCGTM)
Wetting and wicking
Interfacial shear strength (IFSS)
Triple-fiber fragmentation test

ABSTRACT

For improvement of mechanical property and manufacturing efficiency of fiber reinforced composites, wettability, which was affected by temperature, viscosity, the pressure of resin injection, fiber volume fraction, fiber array, and so on, was important factor, which had been focused many researchers. Although the wettability during manufacturing processing was usually evaluated by the permeability, it does not contain the surface energies for the fiber and matrix. Using innovative CF tow capillary glass tube method (TCGTM), this study investigated the wetting, wicking and interfacial properties for three type CFs reinforced epoxy composites combined with a triple-fiber fragmentation test. The CFs TCGTM was performed to evaluate wettability and wicking of CF tow with epoxy resin by measuring height of impregnated epoxy front in capillary tube more practically. After curing the specimens, contact angle between CF and epoxy was measured using FE-SEM photos directly. Wetting and wicking were also evaluated by measuring the impregnated length of epoxy droplets on CF tow, and compared with result by CF TCGTM. From all of the relating tests, the 50C type CF exhibited better wetting and wicking than 60E type CF and the desized CF. Interfacial shear strength (IFSS) were evaluated using a triple-fiber fragmentation test for three different type CFs. Better IFSS of the 50C type CF was consistent with wetting and wicking results by CFs TCGTM. A new innovative CF TCGTM can be applicable for conventional CF reinforced epoxy composites more practically by combining with micromechanical test for the IFSS between single CF and epoxy mainly.

1. Introduction

One of the advantages of polymer material exhibited which products can be manufactured quickly by the injection process [1]. In the case of this material, however, poorer thermal and mechanical properties exhibited than metal and ceramic materials, and it was tried to use composite materials with nanoparticles and fiber reinforcements [2,3]. In current, polymer-based composite has been studied to improve mechanical properties to apply for many industries such as urban air mobility [4]. To improve the mechanical properties of polymer-based composite for structural materials, the fiber reinforcement was more suitable than nanomaterials, and it was manufactured generally by the injection molding with thermoplastic resin [5].

The fiber-reinforced composites (FRC) had to manufacture more quickly and elaborately with a near-zero defect rate [6]. It was a larger scale and more complex shape than previous case, which was manufactured in parts scales. Many researchers had been focusing on the wettability between fibers and polymer resin to evaluate the manufacturing efficiency of FRC in previous publications [7,8]. The wettability between fiber and polymer resin was an important factor affecting the manufacturing cycle time of the manufacturing process. Improvements in wettability are an essential factor for more rapid manufacture of structural composite and to reduce defects such as non-impregnated areas and delamination [9,10].

The wettability of fiber tows by a polymer resin can be evaluated by permeability and capillary tests. Permeability could be viewed as a measure of the inverse of resistance of a porous medium opposing infusion and fluid flow by a polymer matrix. It was related to the

* Corresponding author. Department of Materials Engineering and Convergence Technology, Gyeongsang National University, Jinju, 52828, Republic of Korea.
E-mail address: jmpark@gnu.ac.kr (J.-M. Park).

https://doi.org/10.1016/j.compscitech.2022.109495
Received 30 August 2021; Received in revised form 26 April 2022; Accepted 30 April 2022
Available online 7 May 2022

porosity (i.e., to fibers volume fraction for a fibrous preform) and it is a macroscopic aspect of the impregnation property [11,12]. In the permeability test, the work of adhesion, which was calculated by surface energies for the fiber and matrix, was not included. The work of adhesion affected on the interfacial properties of composites performance significantly [13,14]. These could be the role for the point of stress concentration, and it could be led to the crack propagation under the lower loading. On the other hand, the capillary is a measure of wicking of resins into fibers, as a porous medium [15,16]. Fiber reinforcements were commonly considered porous media, and they might ideally be approximated as a capillary tube network [17,18]. The testing in these references was related to the surface energy and CA of the resin and fibers and was a microscopic factor of the impregnation property using Washburn's equation [19]. This wetting and wicking were closely related to the surface energies of the fibers and polymer resin.

The wetting and wicking were frequently improved by various surface treatments, such as plasma treatment, sizing agent treatment, etching, oxidation, and so on [20–23]. Introducing enough polar groups on the CF surface, recently as carboxyl, hydroxyl, epoxy and amino, would not merely form chemical reactions with the resin but also enhance CF surface wettability [24–26]. This is likely due to this process being easy to apply even to large size objects with relatively minor damage to fibers compared to most other processes. Wetting and wicking were also related to the interfacial and mechanical properties of fiber-reinforced polymer resin-based composites. An optimum interface can relieve stress concentrations by effectively transferring mechanical stress from the matrix resin to the reinforcements thereby enhancing the performance of the composites [27,28]. Interfacial properties are, commonly evaluated using interfacial shear strength (IFSS) and interlaminar shear strength (ILSS) tests, such as the microdroplet pull-out test [29], the multiple fiber fragmentation test [30,31], the short beam test [32,33], etc.

Several methods were used in this work, including a fiber tow capillary tube with triple-fiber fragmentation test. Improved wettability and interfacial properties were evaluated for CFRP with the different sizing agents on the CFs. The surface energies of epoxy resin and different sizing agent treated CFs were calculated using dynamic and static CAs. Wettability was evaluated using impregnation length variations of the epoxy droplet on the CF tow. A capillary test was used to determine the wettability of epoxy resin to CF tows, with three different type of CFs. The height of the resin flow front was compared and checked using Washburn's equation [18] with advanced contact angle measurements and fiber volume fractions. The IFSS of CF/epoxy composite was calculated using triple-fiber fragmentation test correlated with capillary and wettability results.

2. Experimental

2.1. Materials

T-700 grade CF rovings of 50C and 60E (Toray Inc., Japan) were used as composite reinforcement with different sizing agent treatments. Bisphenol-A epoxy (KFR-121, Kukdo Chem., Korea) with amine hardener (KFH-141, Kukdo Chem., Korea) was used for the matrix. The capillary specimen was made using glass capillary tube (HH.1080801, Heinz Herenz Medizinalbedarf GmbH, Germany).

2.2. Methodologies

2.2.1. Sizing agent extracting method

The sizing agent was extracted by Soxhlet equipment using acetone for 24 h to gain desized CF for reinforcement. One meter of each CF was used to extract the coated sizing agent. After the desizing process, the desized CF and extracted solution with acetone were dried to remove acetone in an oven (OF-22GW, Jeio Tech Co., Ltd., Korea) at 40 °C for 4 h in a vacuum. The weight of extract was measured using an electron balance (FX-200i, A&D Co., Korea). The chemical structures of the sizing agent were analyzed using FT-IR (iS-5, Thermo Fisher Scientific Co., U.S.A.) to compare with the sizing agents on 50C and 60E.

2.2.2. CFs TCGTM

The capillary test was performed shows the dynamic CA measuring instrument (DCAT 11, DataPhysics Instruments GmbH, Germany) used in the Capillary Test (Supplementary Fig. 1). The specimens were manufactured from dimethyldichlorosilane (DDS) (SID4120.1, Gelest, Inc., U.S.A.) treated glass capillary tube (1.1 mm inner diameter, HSU-2900000, Paul Marienfeld GmbH, Germany) which was filled with CF to 50 vol% with different sizing agents. The capillary tube was treated to a hydrophobic surface using DDS to decrease the effects of the capillary results. The glass capillary tube was dipped in 1 vol% DDS dissolved in toluene at room temperature for 24 h. The glass capillary tube was rinsed using deionized water and dried in an oven at 40 °C for 24 h. The glass capillary tube with CF tow was just touched on the surface of epoxy resin to impregnate epoxy resin toward CF tow. The variation in weight of the specimens was measured and the experimental height of resin impregnation was observed *in situ,* using a USB microscope. The height of resin impregnation was compared with the calculated height using Washburn's equation [18].

$$h^2(t) = \left\{\frac{(cr)}{2}\right\}\frac{\gamma_L \cos\theta_a}{\eta}t \tag{1}$$

where h is the height of resin impregnation and c is a parameter taking into account tortuosity. R is the mean porous radius and θ_a is the apparent advancing CA. γ_L is the liquid surface tension of the epoxy resin and η is the viscosity of the epoxy resin.

2.2.3. Wettability test between CFs and epoxy matrix

The wettability between CFs and epoxy resin was determined using the work of adhesion, W_a, diameter variation of CF tow, static CA variation of the epoxy droplet, and the capillary test. The amounts of CAs of CFs and epoxy were measured using four different solvents (i.e., distilled water, formamide, ethylene glycol, and diiodomethane) by dynamic and static CAs. Ten CFs were used to measure the dynamic CA more accurately because the weight of CF was too small (Supplementary Fig. 2(a)). The contact angle was calculated using Young's equation [34]:

$$\gamma_S - \gamma_{SL} = \gamma_L \cos\theta \tag{2}$$

where γ_L, γ_{SL}, and γ_S are the liquid surface tension, the solid/liquid interfacial energy, and the solid surface energy, respectively. The total surface energy, γ^T, is the sum of the Lifshitz-van der Waals component, $\gamma^{LW}$and the acid-base component, γ^{AB}. The calculation of these components, following the modified young-Dupre equation [35] of the work of adhesion, W_a can be expressed as:

$$W_a = \gamma_L(1+\cos\theta) = 2\left(\gamma_L^{LW}\gamma_S^{LW}\right)^{\frac{1}{2}} + 2\left[\left(\gamma_S^-\gamma_L^+\right)^{\frac{1}{2}} + \left(\gamma_S^+\gamma_L^-\right)^{\frac{1}{2}}\right] \tag{3}$$

A commonly-used approach in considering solid surface energies is to express them as the sum of dispersive and polar components which can influence the work of adhesion,W_a between the surface of the reinforcement material and the matrix. To determine the polar and dispersive surface free energies, the Owens-Wendt equation [36] is used, expressed as:

$$W_a = \gamma_L(1+\cos\theta) = 2\left(\gamma_S^d\gamma_L^d\right)^{\frac{1}{2}} + 2\left(\gamma_S^p\gamma_L^p\right)^{\frac{1}{2}} \tag{4}$$

where γ_L,γ_L^d, and γ_L^p are known for testing liquids and γ_S^p and γ_S^d can be calculated

from the measured contact angles. Based on the surface energy of the material the work of adhesion between the CFs and epoxy resin was obtained to predict the improvement in interfacial adhesion. The

impregnation length variation of epoxy resin was measured using a USB microscope (Dino-Lite AM4815, AnMo Electronics Co., Taiwan). A one mL epoxy droplet was laid down on the CF tow and impregnation length was measured in-*situ* (Supplementary Fig. 2(b)).

2.2.4. Single fiber tensile test of CFs

The single fiber tensile test was performed to determine the mechanical properties of CFs with different sizing agent content. A single fiber was attached on a paper frame using epoxy adhesive (Huntsman Co., U.S.A.) to hold the specimens to the tensile test zig. The gauge length of the specimens and the strain rate were set to 20 mm and 0.5 mm/min on the UTM (H1K–S, Lloyd Instruments Ltd., U.K). The test was performed 30 times for each condition. The tensile test results were arranged using a Weibull distribution to compare the degree of damage of the CFs during the sizing and desizing processes. The test results were statistically analyzed using both uni- and bimodal Weibull distributions. Fiber failure analysis for the unimodal cumulative Weibull distribution function based on one type of defect is

$$F(t) = 1 - \left\{ p\, exp\left[-\left(\frac{t}{\alpha_1}\right)^{\beta_1} \right] + q\, exp\left[-\left(\frac{t}{\alpha_2}\right)^{\beta_2} \right] \right\} \tag{5}$$

$$p + q = 1$$

where p and q are the portions of the low and high strength population while α_1, β_1 and α_2, β_2 are the scale and shape parameters for the low and high strength portions, respectively [23].

2.2.5. IFSS measurement of tripe-CFs/epoxy composites by a fragmentation test

The IFSS of the CF/epoxy composites was determined by a triple fiber fragmentation test for the different sizing agent contents. The three different type CFs were arrayed into tensile test specimen forms in a silicon mold. A one mm feeler gauge was used to control the gap between the CFs and fixed using scotch tape. The epoxy resin was filled into the silicon mold and cured at 80 °C for 6 h using an autoclave. Tensile stress was applied uniaxially along the fiber axis of the specimens. Fiber fractures occur because the tensile stress was transferred to the fiber from the matrix through the interface. The fiber fracture progresses as the shorter fibers to longer fiber failure until no fiber breaks occurred. The fragment length was measured using an optical microscope. Equation (6) for determining IFSS, using the Weibull distribution for aspect ratio, as modified by Drzal [37]. Since the distribution of fragment lengths was observed experimentally, this relationship has been altered to reflect Weibull statistics in the form

$$IFSS = \frac{\sigma_f}{2\alpha} \bullet \Gamma\left[1 - \frac{1}{\beta}\right] \tag{6}$$

w here α and β are scale and shape parameters of Weibull distribution for aspect ratio, (l_c/d), and Γ is the gamma function.

3. Results and discussion

3.1. Mechanical and chemical properties of CF with three different type CFs

Fig. 1(a) exhibits the extracted sizing agent weights from the desized, 60E, and 50C type CFs using the acetone boiling method. The weight of the desized sizing agent was nearly zero since all sizing agents was extracted from CF. The weight extracted from the 50C type CFs exhibited the twenty-one times more than the case of 60E type CFs. In the FE-SEM photos of Fig. 3(a), the sizing agent was removed from CF surface but some grains were observed on CF surface. However, the agglomerated lumps of the coated sizing agent exhibited for both 60E and 50C type CFs. The size of the agglomerated lumps of 50C type CF was larger than 60E type CF due to more coated sizing agent amounts. Fig. 1(b) exhibited the FT-IR peaks of the two sizing agents, which were extracted from 50C to 60E type CFs, respectively. Since typical peaks were almost identical for both peak cases, it was considered that 60E and 50C types CFs were treated using the same sizing agent with only different contents.

Fig. 2 and Table 1 show the Weibull distribution of the diameter and tensile strength of CFs with different sizing agents. In Fig. 2(a), the diameters of CFs increased from 6.49 μm to 7.27 μm with increasing the amount of sizing agent. The desized CFs exhibited a nearly linear trend as unimodal distribution. As the amount of the sizing agent gradually increased, however, both trends in behavior appeared to be fit by two lines as bimodal distributions. It can be because the diameter of CFs was not uniform due to the treated sizing agents on CF surface. In Fig. 2(b), the tensile strength of the CFs seemed to be rather similar for the two

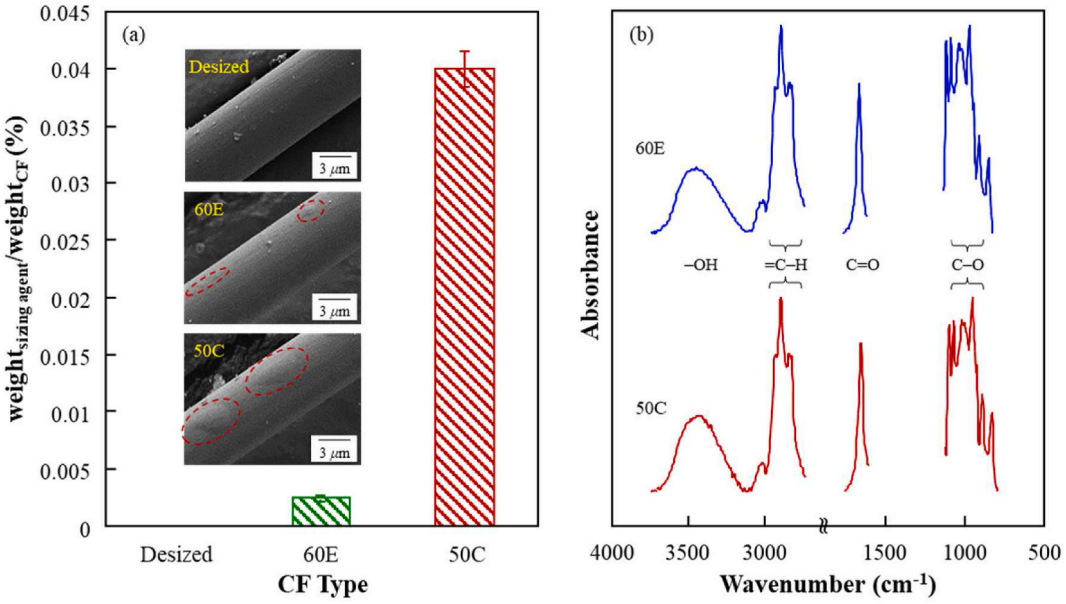

Fig. 1. Sizing agent analysis of CFs with three different type CFs: (a) extracted sizing agent weight; and (b) FT-IR spectra.

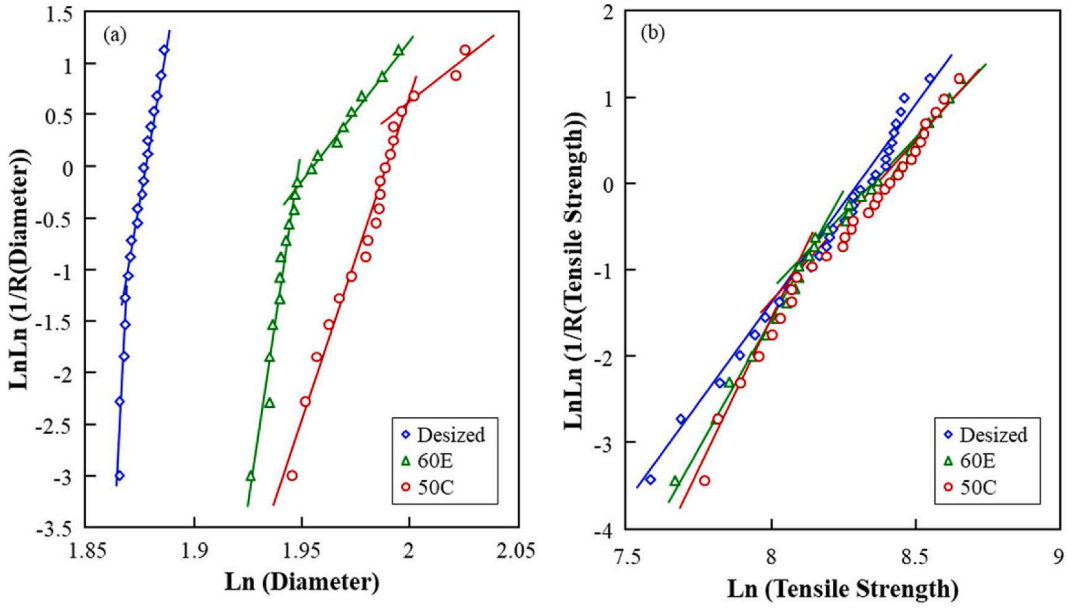

Fig. 2. Mechanical properties of CF with three different type CFs: (a) diameter of CFs; and (b) tensile strength.

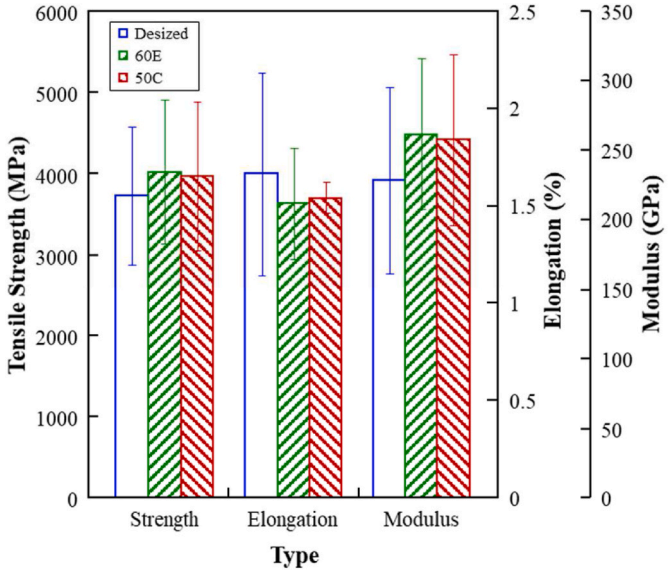

Fig. 3. Comparison of mechanical properties of three different type CFs.

different sizing agents. Although the CFs were known to be not significantly damaged by the sizing treatment process, the desizing process with the boiling acetone cause noticeable damage to the CFs [38,39].

Fig. 3 exhibits the comparison of mechanical properties of CFs with different sizing agent contents. Tensile strength and modulus of 60E and 50C CFs showed rather higher comparing to that the desized CFs, whereas the elongation of the desized CF was larger than those of 60E and 50C CFs. It can be because the sized CFs can provide the healing of defects on the CF surface effective [38–40]. Table 1 showed the comparison of unimodal and bimodal distributions of diameter and tensile strength for three type CFs. Shape parameter from uni- or bimodal distributions can provide the information on the standard deviation of tested diameter and tensile strength. High shape parameter, β, of desized diameters means statistically more uniform distribution of diameter after desizing comparing to 60E and 50C cases for both uni- and bimodal distributions. However, there was no typical trend of shape parameter of tensile strength.

3.2. Wettability of CF/epoxy composites with three different type CFs

Fig. 4 shows the surface energy and work of adhesion, W_a of CF and epoxy for the different sizing agent conditions. The polar term of the surface energy increased from 7.5 to 12 dyne/cm as the amount of sizing agent increased while remaining relatively disperse term. However, the work of adhesion increased from 45.9 to 47.2 dyne/cm even though meaningful difference of the surface energy polar term. The polar surface energy appears to be associated with the increased hydroxyl group as shown by the FT-IR peaks in Fig. 1(b). These observations were also consistent with the fact that the 50C type CF and epoxy resin exhibited better interfacial properties than the 60E cases. Surface energy and work

Table 1
Mechanical properties and diameter of CF with three different type CFs.

Unit	CF Type	Property	Unimodal		Bimodal				Etc
			α^a	β^b	α_1	β_1	α_2	β_2	
Diameter (μm)	Desized	6.49 (0.05)	6.51	150.3	6.51	162	6.53	195	
	60E	7.07 (0.14)	7.14	50.6	6.99	161 -	7.25	61.4	
	50C	7.27 (0.15)	7.34	50.7	7.28	67.1	7.56	58.5	
Tensile Strength (MPa)	Desized	3722 (847)	4091	4.69	3993	4.4	5113	11.5	
	60E	4017 (887)	4374	4.57	3281	12.94	4880	7.18	
	50C	3962 (912)	4330	4.62	2964	8.25	4664	7.17	

1) Standard deviation (SD).
[a] Scale parameter for fiber strength.
[b] Shape parameter for fiber strength.

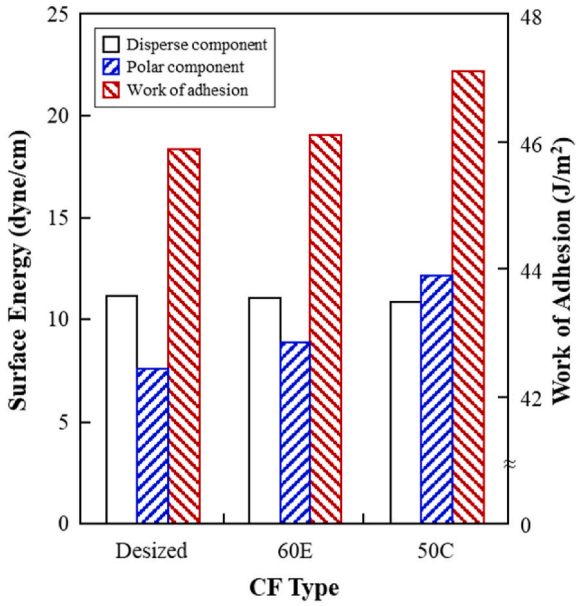

Fig. 4. Surface energies and work of adhesion, W_a with three different type CFs.

of adhesion for single CF and epoxy matrix system were correlated with the interfacial adhesion of more practical multiple CFs and epoxy matrix as well as tri-CFs fragmentation test in the 3.3 section [41,42].

Fig. 5 shows the epoxy droplet size and impregnation length variations under wettability test for the CF/epoxy composite with three different sizing agent conditions. As shown Fig. 2(b), more practical test was performed by measuring epoxy droplet size and impregnation length in the CF tow specimen comparing to the single CF and epoxy system. Initially, the epoxy droplet size and impregnation length increased steeply as the epoxy droplet was spread on the CF tow. At over 1–2 min, however, the epoxy droplet size decreased due to epoxy becoming impregnated into the CF tow steadily. The impregnation length increased continuously as the elapsing time increased due to the epoxy resin spreading and impregnating into CF tow. This result also was correlated to the trend of epoxy droplet size intimately but rather

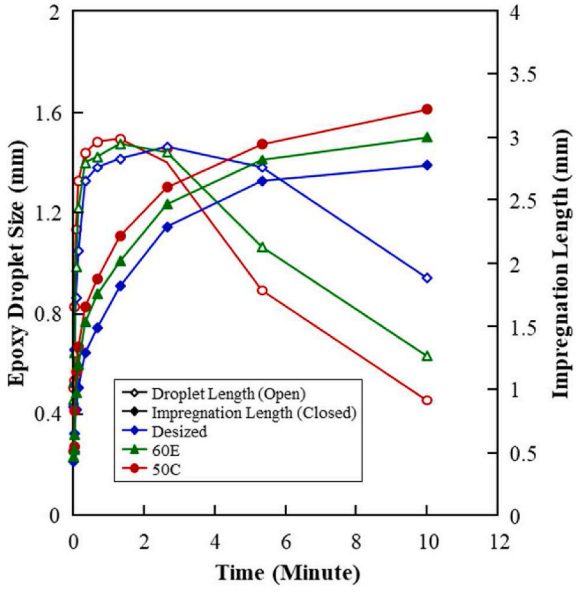

Fig. 5. Droplet and impregnation lengths of epoxy resin with three different type CFs.

differently.

Fig. 6(a) shows the result from capillary test of CFs and epoxy resin with different sizing agent contents. The weight of specimens increased rapidly as the CF contacts the epoxy resin further. The weight of 50C type CF increased more rapidly than another 60E and dezised CFs due to the difference in surface energy. The 50C type CFs was the best maximum weight of the specimen than other two CFs types because the 50C type CF was impregnated with more epoxy resin than other two CFs. Fig. 6(b) shows the height of the resin flow front with different fiber volume fractions to determine the '*r*' factor in equation (1). As the fiber volume fraction of CF *versus* epoxy resin increased, the height of the resin flow front decreased because the CFs were more "stuck" to each other and less capillary effect. The height of the epoxy resin flow front was different for three different type CFs. The height of the resin flow front of 50C type CFs was highest than the desized and 60E CFs cases. It was predicted that the interfacial properties between CFs and epoxy resin can be dependent upon the wettability based on the surface energy of CFs as well as capillary effect of CF tow volume fractions.

As shown in Fig. 6(c), after curing capillary specimens, the meniscus between the epoxy resin and the CFs surface was observed using FE-SEM to determine the interfacial properties between the CFs and the epoxy resin used to ascertain the 'cos θ_a' factor in equation (1). The contact angle at the meniscus decreased from 70° to 24°, as the amount of sizing agent increased on the CF surface. This result indicates that the wettability between the epoxy resin and CFs was improved as the amount of sizing agent increased. The low contact angle implies that the attraction between two materials was higher due to the surface energies, and it causes increased interfacial adhesion and wetting properties [40–44].

Fig. 7 shows schematic arrangements of wettability of CF tow for three different type CFs. The desized CFs exhibited the highest contact angle and the lowest height of epoxy resin among three different CFs. This can be because reactive sites including hydrogen bonding might existed little on the surface of the desized CFs. On the other hand, there were reactive sites and functional groups for 60E and 50C CFs types. The lower contact angle and higher height of epoxy resin exhibited because CFs surface with proper sizing agent has more compatibility and attraction with the epoxy resin [42,43].

3.3. IFSS of CF/epoxy composites for three different type CFs

Figs. 8 and 9 show panorama photographs of specimens after triple fiber fragmentation testing and their IFSS comparison using Drzal's equation (6). The CF fragment distributions to obtain IFSS were shown in Fig. 8 as an advanced single fiber fragmentation test. The CF fragment length decreased and a greater number of CF fragment, the IFSS increased. The 50C type CF exhibited better interfacial properties with the epoxy matrix than the other fibers. Fig. 9 shows the IFSS for the CF/epoxy composites with three different CFs, calculated using Drzal's equation above. The IFSS exhibited the best for 50C type CFs than the desized and 60E CFs cases. As shown in the schematic arrangement of the interface between epoxy and CFs in Fig. 7, the reactive groups exist little on the desized CF, and as a result, there was relatively poor interfacial adhesion between the CF surfaces and the epoxy chains. As the sizing agent layer increased, however, more hydroxyl groups and other carboxyl groups existed on the CF surface and hydrogen bonding could occur between the CF surfaces and epoxy chains [44,45].

4. Conclusions

Innovate wettability of CF tows in epoxy resin was evaluated using a capillary method, and the interfacial properties evaluated using triple CF fragmentation test were correlated with micromechanical technique for three different type CFs. The two-typed CFs were coated using identical coupling agent and more amount of sizing agent existed in 50C CF type. Desized CF exhibited the lowest mechanical property, and it could be due to the acetone boiling process to delete the sizing agent.

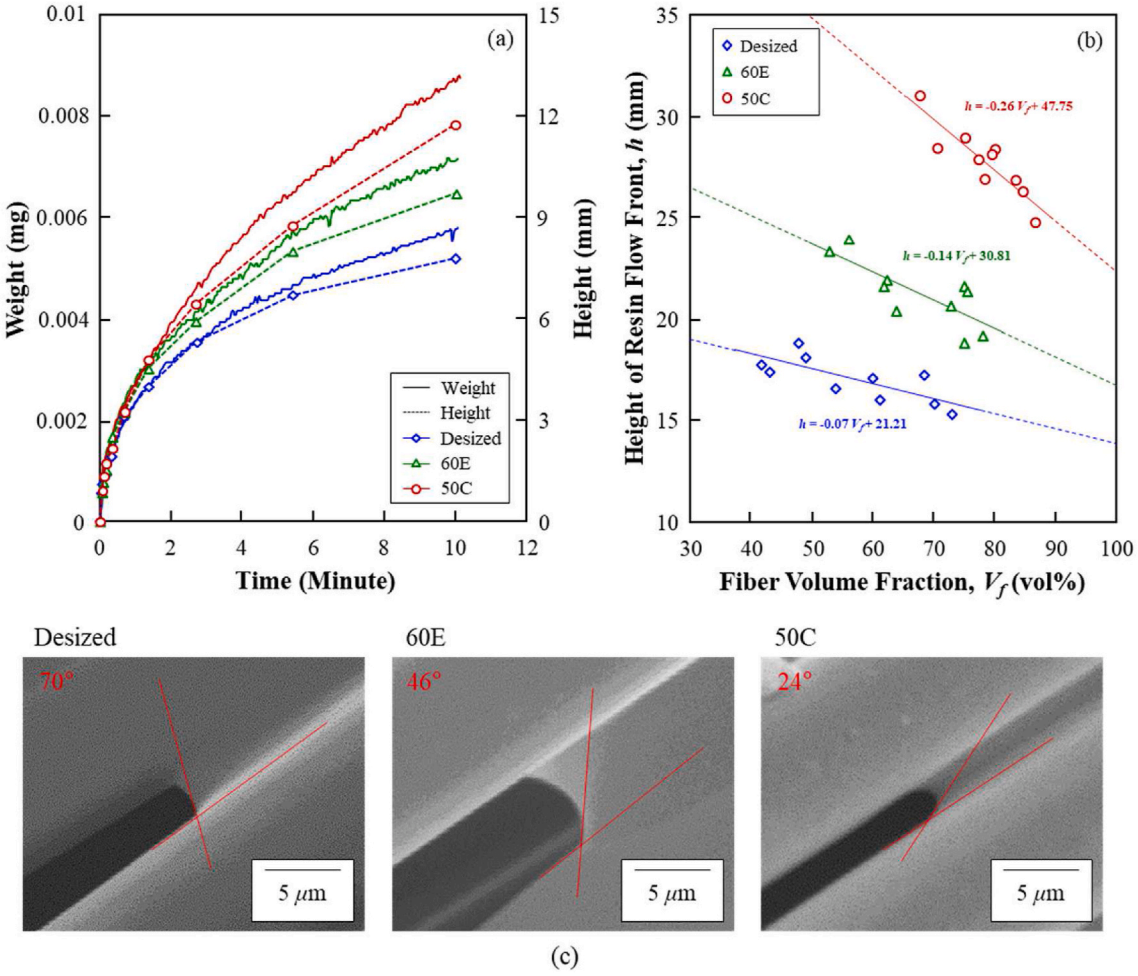

Fig. 6. Capillary test of CF tow and epoxy resin for three different type CFs: (a) weight *versus* time; (b) height of resin flow front *versus* fiber volume fraction; and (c) contact angle between CFs and epoxy resin *via* FE-SEM.

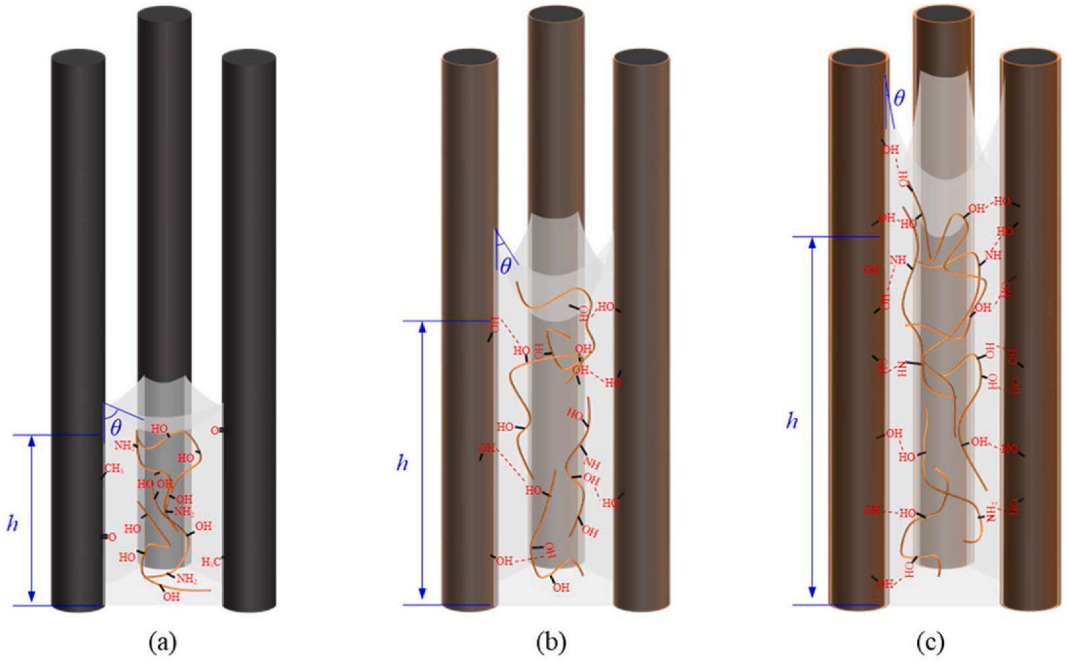

Fig. 7. Schematic plots of wettability of CF tow with three different type CFs: (a) desized; (b) 60E; and (c) 50C.

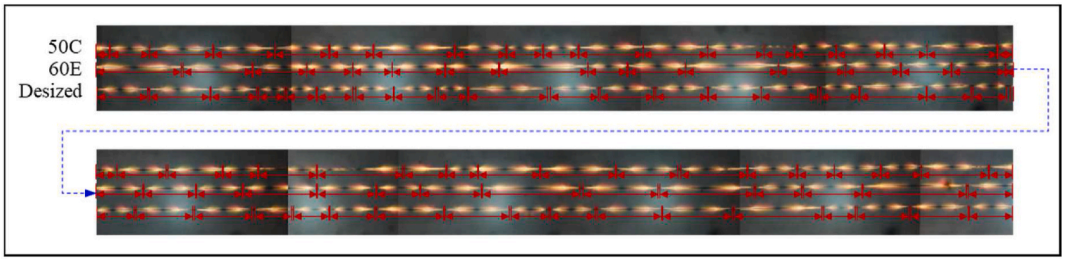

Fig. 8. Panorama photograph of triple fiber fragmentation specimen with three different type CFs.

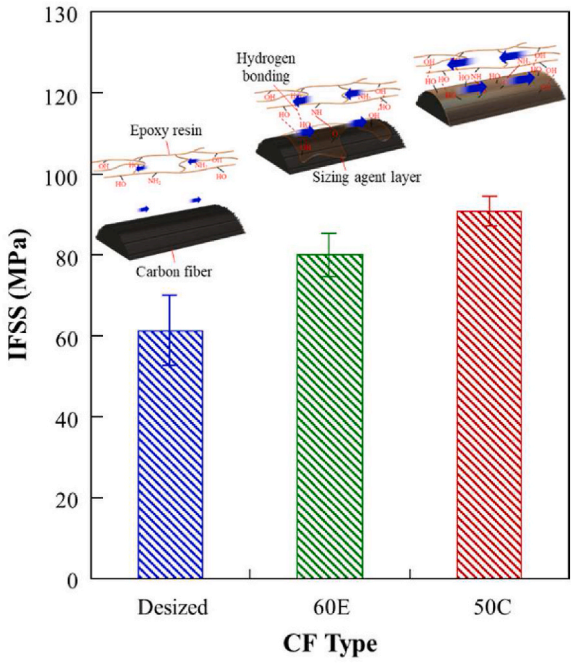

Fig. 9. The IFSS of CF/epoxy composite with three different type CFs.

The 50C type CF exhibited the best W_a and wettability and interfacial properties due to high polar surface energy. In the wettability test, the impregnation length of 50C type CF increased while the epoxy droplet size decreased most rapidly. In the capillary with CF tow test, its weight and height were the largest as CFs fraction increased. The 50C type CF exhibited the best interfacial properties, e.g. the calculated IFSS. It appears that all these test results indicate that 50C type CF is a superior reinforcing filler. In wettability results, the 50C type CF exhibited the best wettability, and the capillary test applied from Washburn's equation can be applicable to real CF tow in epoxy resin composite system practically.

Compliance with ethical standards

The authors declare that they have no conflict of interest.

CRediT authorship contribution statement

Jong-Hyun Kim: Writing – original draft, Data curation, Visualization, Formal analysis. **Dong-Jun Kwon:** Formal analysis, Writing – review & editing. **Lawrence K. DeVries:** Formal analysis, Writing – review & editing. **Joung-Man Park:** Formal analysis, Visualization, Writing – review & editing, Visualization, Supervision.

Declaration of competing interest

The authors declare that they have no known competing financial interests or personal relationships that could have appeared to influence the work reported in this paper.

Acknowledgements

This research was supported by Basic Science Research Program through the National Research Foundation of Korea (NRF) funded by the Ministry of Education under Grant No. 2016R1D1A1B01012620; and 2020R1A6A1A03038697.

Appendix A. Supplementary data

Supplementary data to this article can be found online at https://doi.org/10.1016/j.compscitech.2022.109495.

References

[1] H. Fu, H. Xu, Z. Yang, S. Kormakov, D. Wu, J. Sun, Overview of injection molding technology for processing polymers and their composites, ES Mater Manuf 8 (2020) 3–23.
[2] S.M. Shahabaz, S. Sharma, N. Shetty, S.D. Shetty, M.C. Gowrishankar, Influence of temperature on mechanical properties and machining of fibre reinforced polymer composites: a review, Eng. Sci. 16 (2021) 26–46.
[3] J.C.D.M. Neto, N.R.D. Nascimento, R.H. Bello, L.A.D. Vercosa, J.E. Neto, J.C.M. D. Costa, F.R.V. Diaz, Kaolinite review: intercalation and production of polymer nanocomposites, Eng. Sci. 17 (2022) 28–44.
[4] D.M. Bushnell, Prospective futures of civilian air transportation, Eng. Sci. 16 (2021) 5–8.
[5] J. Li, P. Zhang, H. He, S. Zhai, Y. Xian, W. Ma, Y. Wang, Enhanced thermal transport properties of epoxy resin thermal interface materials, ES Energy Environ 4 (2019) 41–47.
[6] J. Zhang, V.S. Chevali, H. Wang, et al., Current status of carbon fibre and carbon fibre composites recycling, Compos. B Eng. 193 (2020) 108053.
[7] S.H. Lim, S.Y. On, H.S. Kim, Y.H. Bang, S.S. Kim, Resin impregnation and interfacial adhesion behaviors in carbon fiber/epoxy composites: effects of polymer slip and normalized surface free energy with respect to the sizing agents, Compos. Appl. Sci. Manuf. 146 (2021) 106424.
[8] H. Zheng, W. Zhang, B. Li, J. Zhu, C. Wang, G. Song, G. Wu, X. Yang, Y. Huang, L. Ma, Recent advances of interphases in carbon fiber-reinforced polymer composites: a review, Compos. B Eng. 233 (2022) 109639.
[9] J.I. Kim, Y.T. Hwang, K.H. Choi, H.J. Kim, H.S. Kim, Prediction of the vacuum assisted resin transfer molding (VARTM) process considering the directional permeability of sheared woven fabric, Compos. Struct. 211 (2019) 236–243.
[10] M. Megahed, S.M. Youssef, S.S. Ali-Eldin, M.A. Agwa, Upgraded mechanical properties of diluent nano-filled glass/epoxy composites fabricated by vacuum assisted resin infusion, Fibers Polym. 22 (2021) 1063–1081.
[11] Q. Ma, Z. Yang, Y. Gu, M. Li, S. Wang, Z. Zhang, Permeabilities along fiber direction of ramie bundles and through-thickness of ramie fabric stack for liquid composite molding, J. Reinforc. Plast. Compos. 36 (2017) 40–52.
[12] D. Salvatori, B. Caglar, H. Teixido, V. Michaud, Permeability and capillary effects in a channel-wise non-crimp fabric, Compos Part A 108 (2018) 41–52.
[13] J.S. Leclerc, E. Ruiz, Porosity reduction using optimized flow velocity in Resin Transfer Molding, Compos Part A 39 (2008) 1859–1868.
[14] V. Michaud, A review of non-saturated resin flow in liquid composite moulding processes, Transport Porous Media 115 (2016) 581–601.
[15] H.N. Vo, M.F. Pucci, S. Corn, N.L. Moigne, W. Garat, S. Drapier, P.J. Liotier, Capillary wicking in bio-based reinforcements undergoing swelling - dual scale consideration of porous medium, Compos Part A 134 (2020) 105893.
[16] B. Caglar, C. Tekin, F. Karasu, V. Michaud, Assessment of capillary phenomena in liquid composite molding, Compos Part A 120 (2019) 73–83.

[17] R. Massodi, K.M. Pillai, Darcy's law-based model for wicking in paper-like swelling porous media, Fluid Mech Transp Phenom 56 (2010) 2257–2267.
[18] E.W. Washburn, The dynamics of capillary flow, Phys. Rev. 17 (1921) 273–283.
[19] M. Abida, F. Gehring, J. Mars, A. Vivet, F. Dammak, M. Haddar, Hygro-mechanical coupling and multiscale swelling coefficients assessment of flax yarns and flax/epoxy composites, Compos Part A 136 (2020) 105914.
[20] F. Liu, Z. Shi, Y. Dong, Improved wettability and interfacial adhesion in carbon fibre/epoxy composites via an aqueous epoxy sizing agent, Compos Part A 112 (2018) 337–345.
[21] Z. Wu, H. Cui, L. Chen, D. Jiang, L. Wang, Y. Ma, X. Li, X. Zhang, H. Liu, N. Wang, J. Zhang, Y. Ma, M. Zhang, Y. Huang, Z. Guo, Interfacially reinforced unsaturated polyester carbon fiber composites with a vinyl ester-carbon nanotubes sizing agent, Compos. Sci. Technol. 164 (2018) 195–203.
[22] R.B. Ashok, C.V. Srinivasa, B. Basavaraju, Study on morphology and mechanical behavior of areca leaf sheath reinforced epoxy composites, Adv Compos Hybrid Mater 3 (2020) 365–374.
[23] J. Yao, Q. Fang, G. Zhang, C. Yang, K. Niu, Effect of hydrophilic-hydrophobic ratio in self-emulsifying amphiphilic epoxy sizing agent on interfacial properties of carbon fibre/epoxy composites, Prog. Org. Coating 143 (2020) 105621.
[24] L. Shi, G. Song, P. Li, X. Li, D. Pan, Y. Huang, L. Ma, Z. Guo, Enhancing interfacial performance of epoxy resin composites via in-situ nucleophilic addition polymerization modification of carbon fibers with hyperbranched polyimidazole, Compos. Sci. Technol. 201 (2021) 108522.
[25] L. Ma, Y. Zhu, P. Feng, G. Song, Y. Huang, H. Liu, J. Zhang, J. Fan, H. Hou, Z. Gao, Reinforcing carbon fiber epoxy composites with triazine derivatives functionalized graphene oxide modified sizing agent, Compos Part B 176 (2019) 107078.
[26] H. Lyu, N. Jiang, J. Hu, Y. Li, N. Zhou, D. Zhang, Preparing water-based phosphorylated PEEK sizing agent for CF/PEEK interface enhancement, Compos. Sci. Technol. 217 (2022) 109096.
[27] C. Lu, J. Wang, X. Lu, T. Zheng, Y. Liu, X. Wang, D. Zhang, D. Seveno, Wettability and interfacial properties of carbon fiber and poly(ether ether ketone) fiber hybrid composite, ACS Appl. Mater. Interfaces 11 (2019) 31520–31531.
[28] J.H. Kim, D.J. Kwon, P.S. Shin, H.S. Park, Y.M. Baek, K.L. DeVries, J.M. Park, Evaluation of interfacial and mechanical properties of glass fiber and p-DCPD composites with surface treatment of glass fiber, Compos Part B 153 (2018) 420–428.
[29] P.S. Shin, J.H. Kim, H.S. Park, Y.M. Baek, D.J. Kwon, K.L. DeVries, J.M. Park, Advanced interfacial properties of glass fiber/dopamine-epoxy composites using a microdroplet pull-out test and acoustic emission, J. Adhes. 97 (2019) 438–455.
[30] J.M. Park, J.W. Kim, K. Goda, A new method of evaluating the interfacial properties of composites, Compos. Sci. Technol. 60 (2000) 439–450.
[31] H.S. Park, P.S. Shin, J.H. Kim, Y.M. Baek, D.J. Kwon, W.I. Lee, K.L. DeVries, J. M. Park, Evaluation of interfacial and mechanical properties of glass, Fibers Polym. 19 (2018) 1989–1996.
[32] A.I. Gagani, A.E. Krauklis, E. Sæter, N.P. Vedvik, A.T. Echtermeyer, A novel method for testing and determining ILSS for marine and offshore composites, Compos. Struct. 220 (2019) 431–440.
[33] A. Gaurav, K.K. Singh, ILSS improvement of quasi-isotropic glass fiber reinforced epoxy laminate enhanced with arc discharged multi-walled carbon nanotube, Mater. Today Proc. 5 (2018) 8638–8644.
[34] A.J. Kinloch, Adhesion and Adhesives, Chapman and Hall, London, 1987.
[35] N. Dilsiz, J.P. Wightman, Colloids and surfaces A: physicochemical and engineering aspects, Colloids Surf., A 164 (2000) 325–336.
[36] D.K. Owen, R.C. Wendth, Estimation of the surface free energy of polymer, J. Appl. Polym. Sci. 13 (1969) 1741–1747.
[37] L.T. Drzal, M.J. Rich, P.F. Lloyd, Adhesion of graphite fibers to epoxy matrices: I. The role of fiber surface treatment, J. Adhes. 16 (1983) 1–30.
[38] J.M. Park, W.G. Shin, D.J. Yoon, A study of interfacial aspects of epoxy-based composites reinforced with dual basalt and SiC fibres by means of the fragmentation and acoustic emission techniques, Compos. Sci. Technol. 59 (1999) 355–370.
[39] J.M. Park, S.T. Quang, B.S. Hwang, K.L. DeVries, Interfacial evaluation of modified Jute and Hemp fibers/polypropylene (PP)-maleic anhydride polypropylene copolymers (PP-MAPP) composites using micromechanical technique and nondestructive acoustic emission, Compos. Sci. Technol. 66 (2006) 2686–2699.
[40] J.H. Kim, D.J. Kwon, P.S. Shin, H.S. Park, Y.M. Baek, K.L. DeVries, J.M. Park, Evaluation of interfacial and mechanical properties of glass fiber and *p*-DCPD composites with surface treatment of glass fiber, Compos Part B 153 (2018) 420–428.
[41] T.T.L. Doan, H. Brodowsky, E. Mäder, Jute fibre/epoxy composites: surface properties and interfacial adhesion, Compos. Sci. Technol. 72 (2012) 1160–1166.
[42] P.S. Shin, Y.M. Baek, J.H. Kim, H.S. Park, D.J. Kwon, J.H. Lee, M.Y. Kim, K. L. DeVries, J.M. Park, Interfacial and wetting properties between glass fiber and epoxy resins with different pot lifes, Colloids Surf., A 544 (2018) 68–77.
[43] S.H. Lim, S.Y. On, H.S. Kim, Y.H. Bang, S.S. Kim, Resin impregnation and interfacial adhesion behaviors in carbon fiber/epoxy composites: effects of polymer slip and normalized surface free energy with respect to the sizing agents, Compos Part A 146 (2021) 106424.
[44] F.M. Zhao, T. Okabe, N. Takeda, The estimation of statistical fiber strength by fragmentation tests of single-fiber composites, Compos. Sci. Technol. 60 (2000) 1965–1974.
[45] J.M. Park, Y.M. Kim, K.W. Kim, D.J. Yoon, Interfacial aspects of electrodeposited carbon fiber-reinforced epoxy composites using monomeric and polymeric coupling agents, J. Colloid Interface Sci. 231 (2000) 114–128.